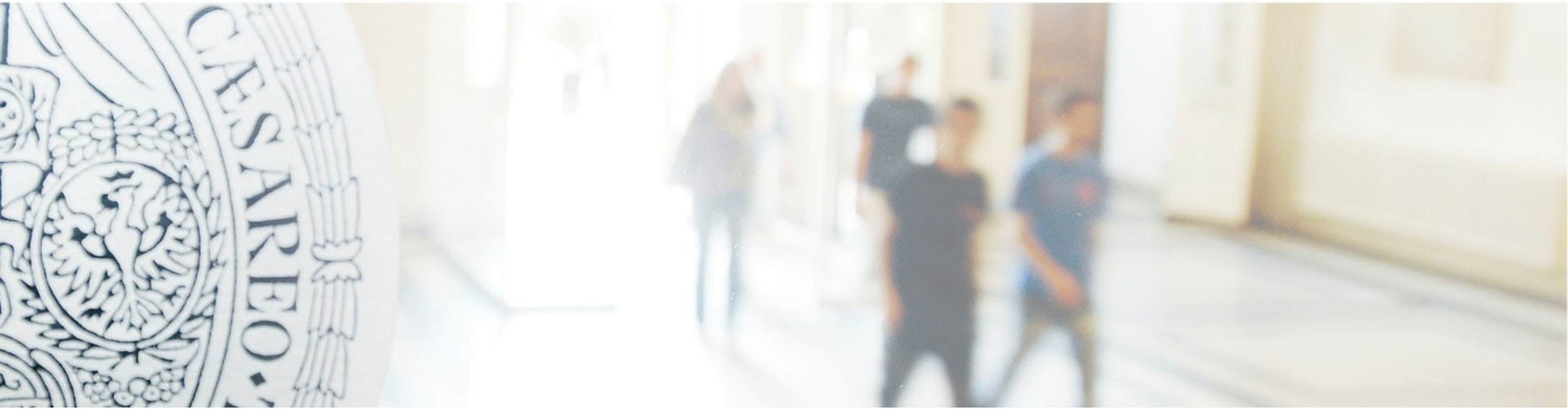

FR-0 jetted active galaxies: extending the zoo of candidate sites for UHECR acceleration.

L. Merten[1], M. Boughelilba[1], A. Reimer[1], P. Da Vela[1],
S. Vorobiov[2], F. Tavecchio[3], G. Bonnoli[4], J.P. Lundquist[2], C. Righi[3]
[1]University of Innsbruck, [2]University of Nova Gorica, [3]Astronomical Observatory of Brera,
[4]Instituto de Astrofísica de Andalucía

ICRC 2021 | Berlin | 13.07.2021

Contents

- FR 0 — Numbers, Luminosities, Host Galaxies, etc.
- SED — Photon target field, magn. field, etc.
- Pacc — Acceleration, Escape, and Losses
- Emax — UHECRs?

Why another class of UHECR accelerators?

FR0-*CAT*atalogue

Fact Box

- Comparable to FR I (radio loud AGNs)
- Less luminous than FR I: $L_{\mathrm{jet}} \approx 10^{42\ldots 43.5}\mathrm{erg/s}$ (based on Heckmann&Best (2014))
- More numerous in the local universe: $n_{\mathrm{FR\,0}} \approx 5 n_{\mathrm{FR\,I}}$ (Baldi&Capetti (2009), Baldi&Capetti (2010))
- Very short jets: $\mathrm{pc} < R_{\mathrm{jet}} < \mathrm{kpc}$ (Baldi&Capetti 2019, Cheng&An 2018)
- Host → slightly less massive ellipticals: $M_{\mathrm{gal}} \approx 10^{8\ldots 9} M_{\mathrm{sol}}$

Spectral energy distribution

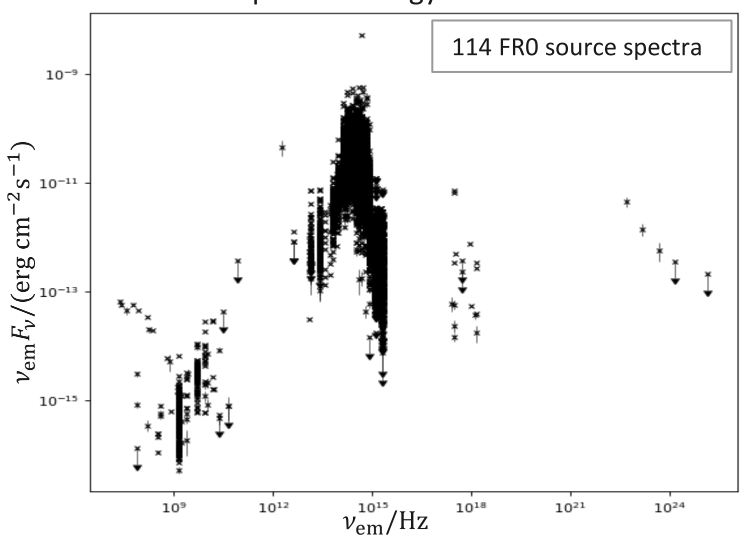

Positions in the sky (Galactic)

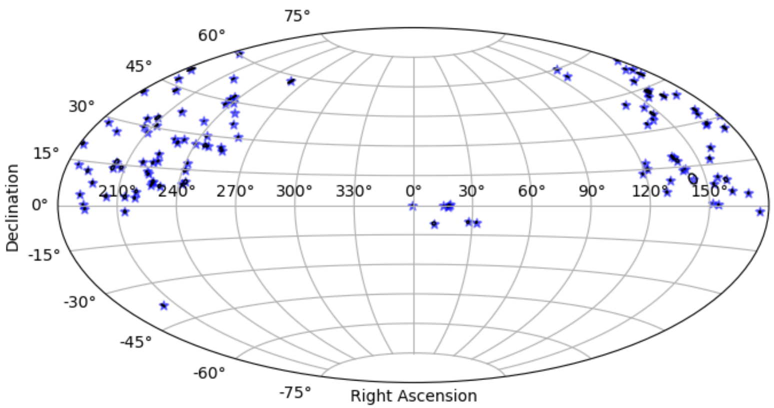

Spectral Energy Distribution (SED)

Goal: Realistic description of the target photon fields

Steps: Ignore γ-ray data (not relevant as targets)
Two components: jet and host galaxy spectrum
Average-by-eye → Not overshooting the data but no accurate modelling

Internal – Jet

Minimal Synchrotron-Self-Compton approach

→Description nuclei target

→Source parameters: B, r_{em}, Γ_j, D

External – Host Galaxy

Diluted blackbody energy spectrum

De-Vaucouleur's radial profile

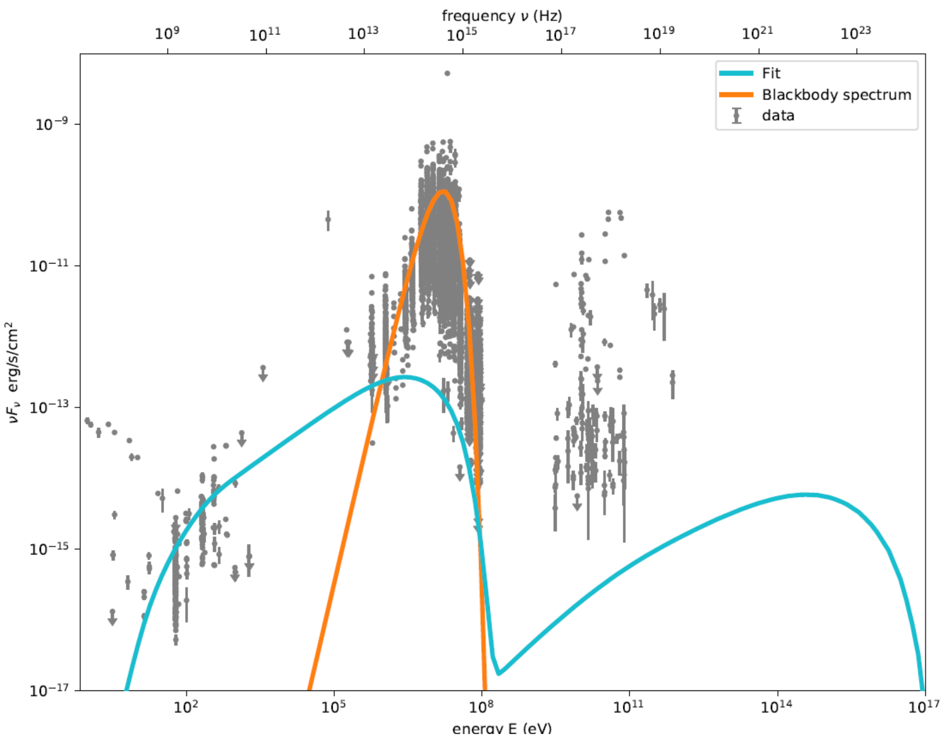

Competing processes

Acceleration

Fermi-I-order

$$\tau_{\mathrm{Bohm}}^{\mathrm{Fermi}} = \frac{20}{3} \frac{E}{u_s^2 qB}$$

Gradual Shear

$$\tau_{\mathrm{Bohm}}^{\mathrm{shear}} = \frac{3}{\Gamma_j^4} \left(\frac{\partial u}{\partial r}\right)^{-2} \frac{Bqc^2}{E}$$

Energy losses

Bethe-Heitler pair production, Photodisintegration, Photo-Meson-Production, Synchrotron radiation

Escape

Advective

$$\tau_{\mathrm{adv}} = \frac{L}{v}$$

Diffusive

$$\tau_{\mathrm{dif}} = \frac{R^2}{2\kappa}$$

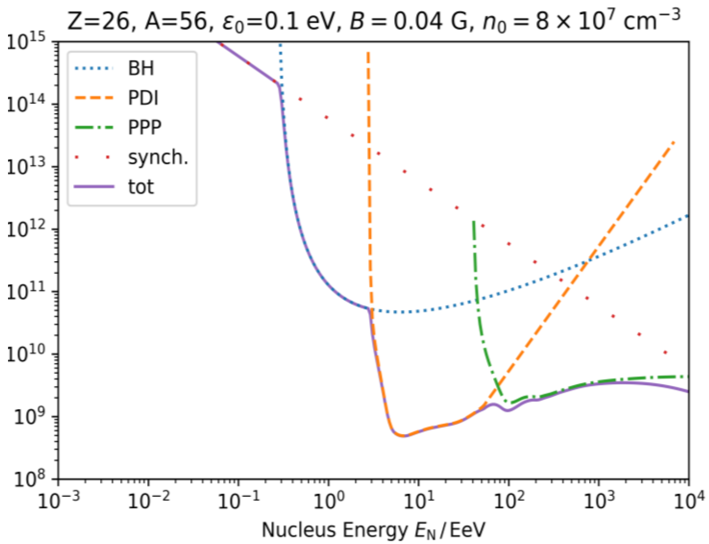

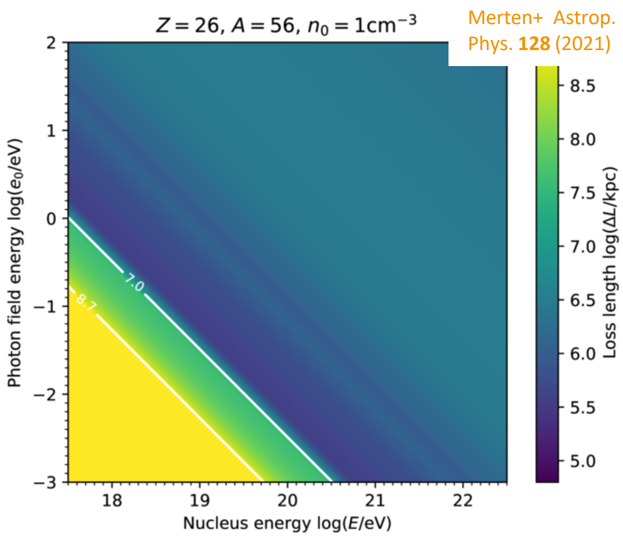

Merten+ Astrop. Phys. **128** (2021)

UHECRs in FR 0 sources

Time scales in source environment – Bohm

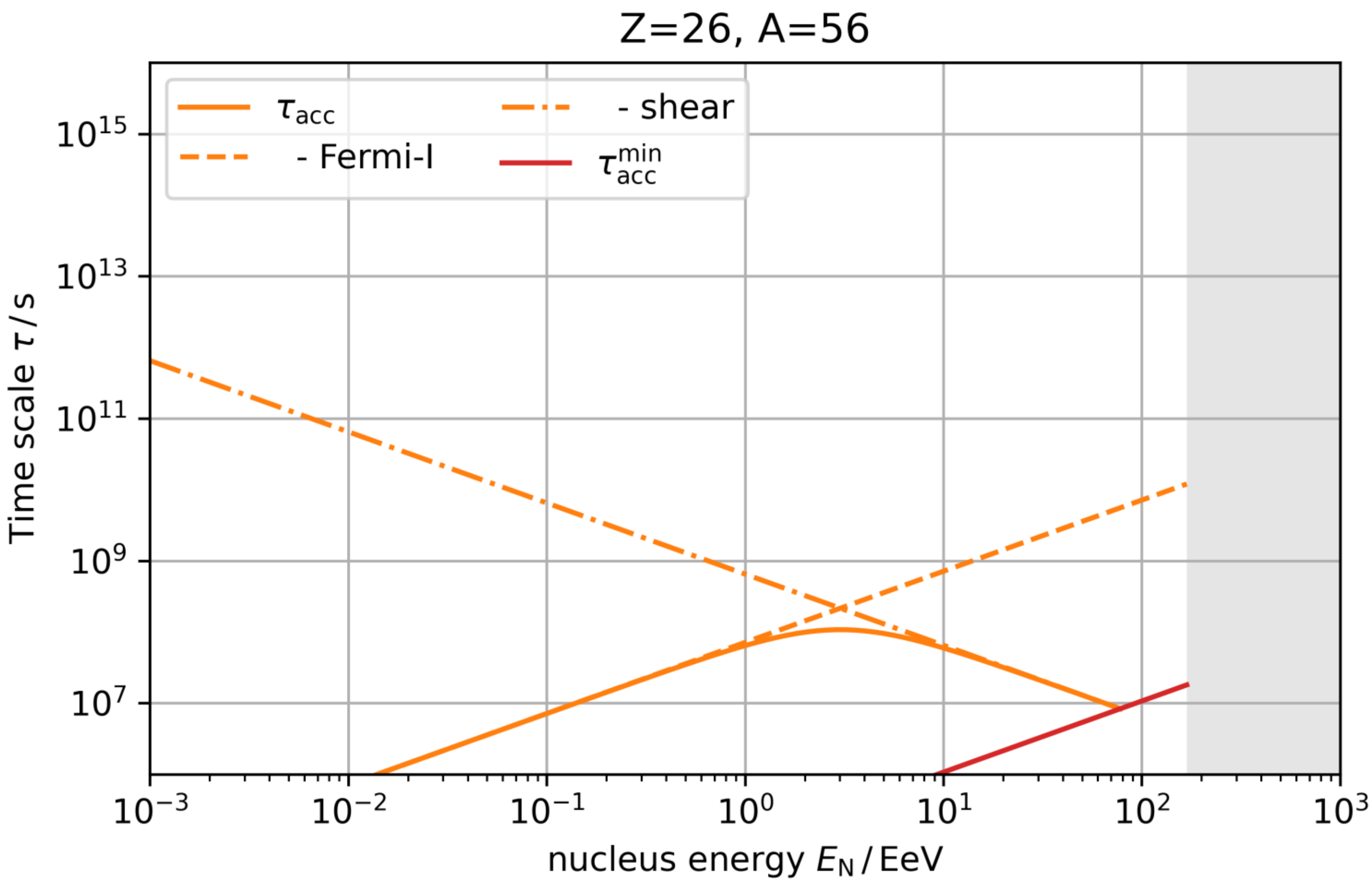

Time scales in source environment – Bohm

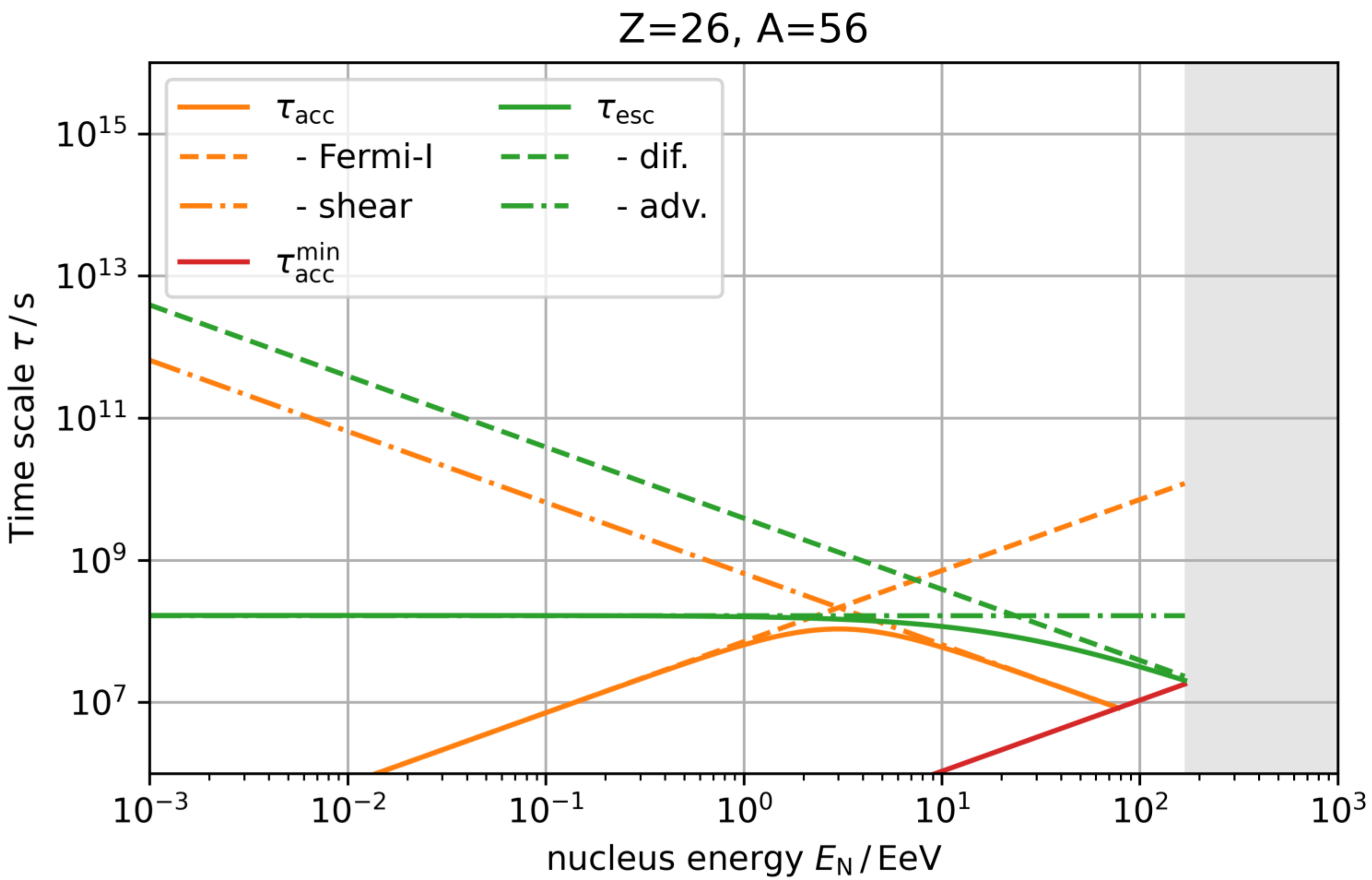

Time scales in source environment – Bohm

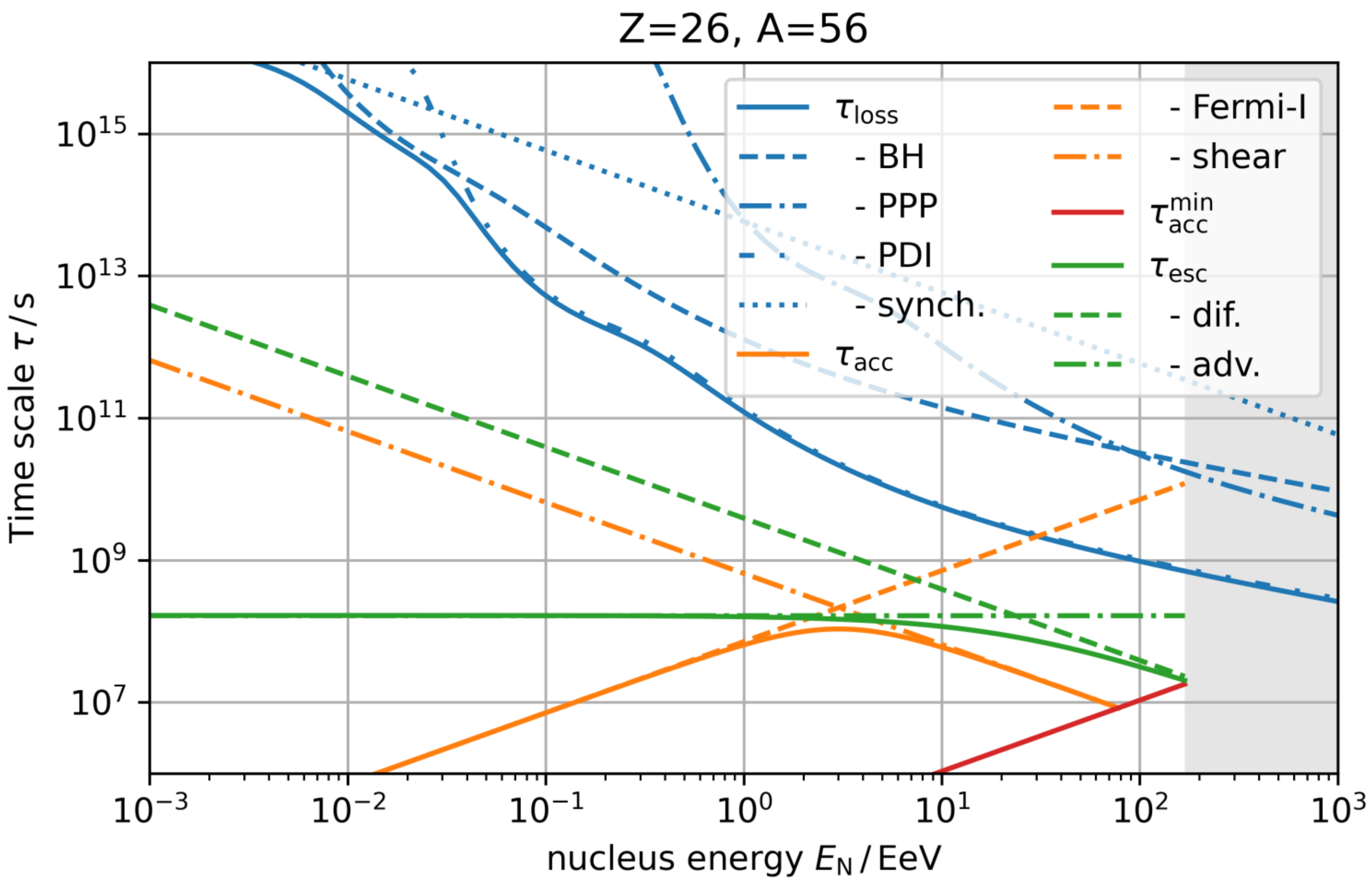

Acceleration Probability

This probability is a measure for the dominance of acceleration:

$$P_{acc} \coloneqq \frac{\sum {\tau_{acc}^{i}}^{-1}}{\sum {\tau_{acc}^{i}}^{-1} + \sum {\tau_{loss}^{j}}^{-1} + \sum {\tau_{esc}^{k}}^{-1}},$$ defining the maximum energy $P(E_{max}^{acc}) = 0.5$

Bohm diffusion ($\kappa \propto E$)

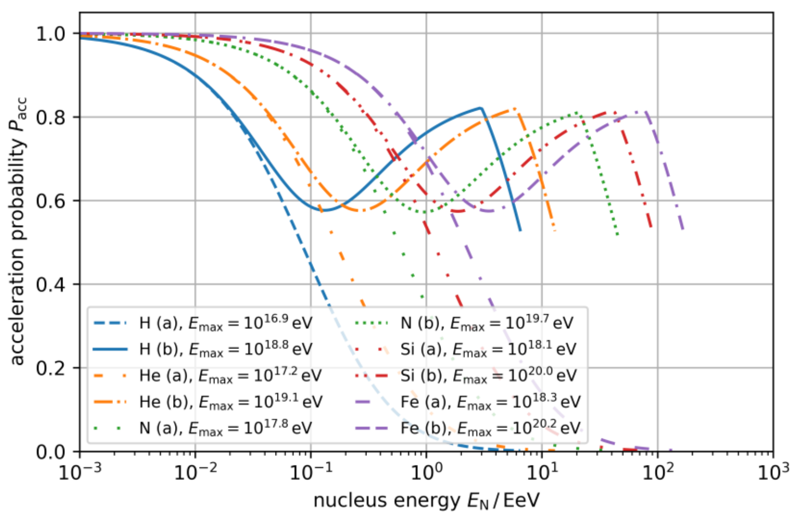

Kolmogorov diffusion ($\kappa \propto E^{1/3}$)

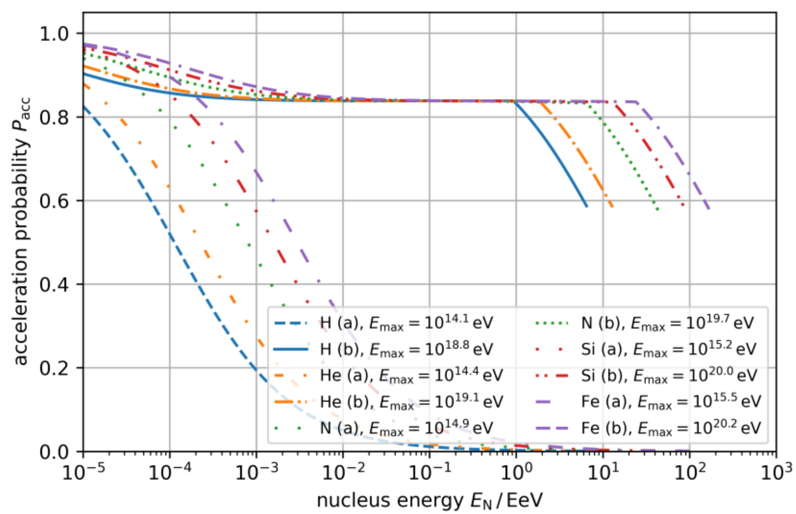

Maximum Energies

Hillas Energy: $E_{max}^{Hillas} = eZBR\beta c \approx 10^{21} Z \left(\frac{B}{\mathrm{G}}\right)\left(\frac{R}{\mathrm{pc}}\right) \mathrm{eV}$

Source Environment: $P(E_{\mathrm{max}}^{\mathrm{acc}}) = 0.5$

$\rightarrow E_{\mathrm{max}} = \min\left(E_{\mathrm{max}}^{\mathrm{Hillas}}, E_{\mathrm{max}}^{\mathrm{acc}}\right)$

Maximum energies

Turb.	Accel.	$\log(E/eV)$					$\langle log(R/V) \rangle$
		P	He	N	Si	Fe	
Bohm	Fermi-I	16.9	17.2	17.8	18.1	18.3	16.91±0.03
Bohm	Hybrid	18.8	19.1	19.6	20.0	20.2	18.82±0.03
Kolm.	Fermi-I	14.1	14.4	14.9	15.2	15.5	14.08±0.02
Kolm.	Hybrid	18.8	19.1	19.6	20.0	20.2	18.82±0.03

SUMMARY & OUTLOOK

FROs can accelerate UHECR

- Hybrid scenario is capable of accelerating UHECR
  - When $\Gamma_j > 1.6$ and $r_{\mathrm{em}} \approx 5 \times 10^{17}\,\mathrm{cm}$
- Gradual shear alone will not work. But pre-acceleration can be different from Fermi-I.
- Pure Fermi-I acceleration + Bohm diffusion
  → Contribution between *knee* and *ankle*
- Turbulence model not significant in hybrid model **if** UHECRs are always diffusive.
- Concrete shock speed not relevant if efficient pre-acceleration is possible.
- Radiative losses play an important role in shaping the emitted CR spectrum.

What comes next?

Modeling of the CR spectra at source

- Including secondaries like γ-rays and photons

Propagation from source to Earth

- See J.P. Lundquist's poster and flash talk

What are beamed counterparts of FR 0s?

How is the jet structured?

Larger sky coverage of FR 0 observations would be beneficial

BACKUP

Time Scales

Acceleration

$\tau = \eta(E, \Theta, \beta, \dots)\frac{\lambda(E)}{v}$ with $\eta \geq 1$ model dependent, v the particle speed, and λ the scattering length

Gradual shear

$$\tau_{\text{acc}}^{\text{shear}} = \frac{1}{4+\alpha}\frac{1}{\tilde{\Gamma}\tau}, \quad \text{with } \tilde{\Gamma} = \frac{1}{15}\left(\frac{\partial u_z(r)}{\partial r}\right)^2 \Gamma_{\text{jet}}^4$$

shows interesting energy dependence $\propto E^{-\alpha}$

Also other pre-acceleration mechanisms are possible, e.g., Fermi-II order, magnetic reconnection, etc.

Limits for gradual shear acceleration

From $\eta \geq 1$ we can calculate the maximum shear accel. energy:

$$\frac{E_{\max}^{\text{shear}}}{E_0} = \left[\sqrt{\frac{5}{3(4+\alpha)}}\left(\frac{c}{\Gamma_{\text{jet}}}\right)^2\left(\frac{\partial u}{\partial r}\right)^{-2}\kappa_0^{-1}\right]^{1/\alpha} Z,$$

for a diffusion coefficient $\kappa(E) = \kappa_0\left(\frac{E}{E_0}\right)^{\alpha}$ and a velocity gradient in the shear flow given by $\partial u/\partial r$, with $\beta_{\text{jet}} = u_0 c$.

Another limit is given by the need of scattering within the shear layer:
$\Delta L > r_{\text{Larmor}}$

Time scales in source environment – Kolmogorov

Normalization of diffusion coefficient is unknown: $\kappa(E) = \kappa_0(^{E}/_{\mathrm{GeV}})^{\alpha}$
→ Assume that particles with Hillas energy can still diffuse
Quite close to isotropic turbulence [Dundovic et al. (2020)]

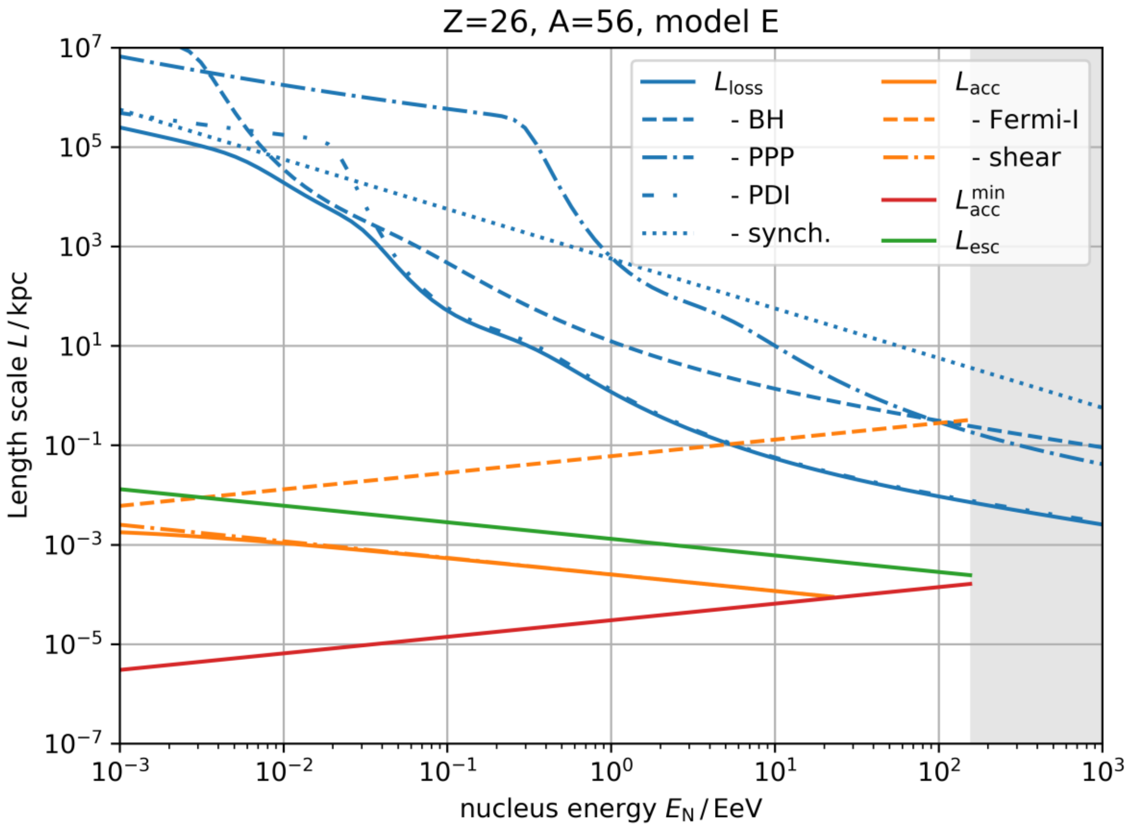

Source list

Sources I

SDSS name	z	NVSS	[O III]	m_r	D_n	sigma_*	C_r	nu_L_r	L[OIII]	M_BH
SDSS J010852.48-003919.4	0.045	10.9	115.7	15.095	2	223	3.43	38.89	39.77	8.3
SDSS J011204.61-001442.4	0.044	17.9	51.2	14.836	1.93	225	2.78	39.09	39.4	8.3
SDSS J011515.78+001248.4	0.045	42.6	84.3	14.554	1.93	241	3.1	39.48	39.63	8.5
SDSS J015127.10-083019.3	0.018	35.7	267.6	13.351	1.97	183	3.03	38.59	39.32	8
SDSS J020835.81-083754.8	0.034	28.4	186.8	13.694	1.93	242	2.97	39.06	39.73	8.5
SDSS J075354.98+130916.5	0.048	7.4	51.5	14.347	2.01	305	3.36	38.77	39.47	8.9
SDSS J080716.58+145703.3	0.029	28.4	63.3	13.712	1.97	215	3.38	38.93	39.13	8.3
SDSS J083158.49+562052.3	0.045	9	93.1	14.514	1.99	216	2.96	38.81	39.68	8.3
SDSS J083511.98+051829.2	0.046	10.1	60.5	14.495	1.93	241	3.24	38.87	39.51	8.5
SDSS J084102.73+595610.5	0.038	8.9	111.9	14	1.97	229	3.28	38.64	39.6	8.4
SDSS J084701.88+100106.6	0.048	23.7	48.4	14.508	1.9	244	3.22	39.28	39.44	8.5
SDSS J090652.79+412429.7	0.027	51.8	143.9	13.808	1.9	189	2.81	39.12	39.42	8
SDSS J090734.91+325722.9	0.049	46.9	35	14.972	1.49	160	2.41	39.6	39.33	7.7
SDSS J090937.44+192808.2	0.028	69.1	342.2	13.877	1.82	234	3.29	39.26	39.81	8.4
SDSS J091039.92+184147.6	0.028	50	78.9	13.298	1.89	195	2.86	39.14	39.19	8.1
SDSS J091601.78+173523.3	0.029	24.5	266.1	13.091	1.91	225	2.35	38.86	39.75	8.3
SDSS J091754.25+133145.5	0.05	22.9	76.3	15.603	1.93	189	3.11	39.3	39.68	8
SDSS J093003.56+341325.3	0.042	33.1	192.2	14.358	1.97	237	3.14	39.31	39.93	8.4
SDSS J093346.08+100909.0	0.011	56.6	567	12.095	2.05	204	3.02	38.34	39.2	8.2
SDSS J093938.62+385358.6	0.046	6.1	74.3	14.864	1.96	197	3.1	38.65	39.59	8.1
SDSS J094319.15+361452.1	0.022	75.1	583.4	13.132	1.81	175	3.15	39.1	39.85	7.9
SDSS J100549.83+003800.0	0.021	24.1	321.5	13.604	2.01	296	3.36	38.55	39.53	8.8
SDSS J101329.65+075415.6	0.046	7.8	137	14.333	2.04	272	3.21	38.76	39.86	8.7
SDSS J101806.67+000559.7	0.048	14.3	781.8	14.965	1.57	156	3.04	39.07	40.66	7.7
SDSS J102403.28+420629.8	0.044	6	39.9	14.652	1.86	204	3.17	38.6	39.28	8.2
SDSS J102511.50+171519.9	0.045	10.2	61.1	13.89	2	309	3.26	38.85	39.48	8.9
SDSS J102544.22+102230.4	0.046	76.7	57.6	14.405	1.93	246	3.02	39.75	39.48	8.5
SDSS J103719.33+433515.3	0.025	132.2	326.4	13.226	1.92	227	3.35	39.44	39.68	8.4
SDSS J103952.47+205049.3	0.046	6.9	126.6	14.38	1.91	202	3.14	38.71	39.83	8.1
SDSS J104028.37+091057.1	0.019	68.5	376.4	12.528	1.93	220	3.12	38.94	39.54	8.3

Sources II

SDSS name	z	NVSS	[O III]	m_r	D_n	sigma_*	C_r	nu_L_r	L[OIII]	M_BH
SDSS J104403.68+435412.0	0.025	32.4	126.1	13.427	1.86	213	3.27	38.84	39.28	8.2
SDSS J104811.90+045954.8	0.034	49.1	313.2	13.597	1.82	196	2.99	39.3	39.96	8.1
SDSS J104852.92+480314.8	0.041	19.2	990.9	14.183	1.77	197	2.87	39.05	40.62	8.1
SDSS J105731.16+405646.1	0.025	44.8	189.5	12.916	2	283	3.08	38.98	39.46	8.7
SDSS J111113.18+284147.0	0.029	41.1	196.5	13.48	1.92	216	2.89	39.07	39.6	8.3
SDSS J111622.70+291508.2	0.045	71.5	86	13.773	2	276	2.91	39.71	39.64	8.7
SDSS J111700.10+323550.9	0.035	17.6	298.7	13.905	1.86	204	3.28	38.87	39.95	8.2
SDSS J112029.23+040742.1	0.05	7.5	142	14.276	1.97	230	2.41	38.81	39.95	8.4
SDSS J112256.47+340641.3	0.043	16.6	199.3	13.477	2.01	270	3.23	39.02	39.96	8.7
SDSS J112625.19+520503.5	0.048	9	85.2	15.336	1.93	172	3.39	38.87	39.7	7.9
SDSS J112727.52+400409.4	0.035	13.8	178.4	14.749	1.94	144	3.48	38.76	39.72	7.6
SDSS J113449.29+490439.4	0.033	33	61.2	13.183	2	299	3.33	39.1	39.22	8.8
SDSS J113637.14+510008.5	0.05	9	35.7	14.818	1.93	223	3.39	38.9	39.35	8.3
SDSS J114230.94-021505.3	0.047	8.8	73.8	14.385	1.92	216	3.04	38.84	39.62	8.3
SDSS J114232.84+262919.9	0.03	42	39.3	13.028	2.02	324	3.2	39.12	38.95	9
SDSS J114804.60+372638.0	0.042	29.1	54	13.818	1.89	281	3.18	39.25	39.37	8.7
SDSS J115531.39+545200.4	0.05	31.2	94.1	14.869	1.96	236	3.16	39.43	39.77	8.4
SDSS J120551.46+203119.0	0.024	89.9	126.5	13.776	1.94	190	3.27	39.24	39.24	8
SDSS J120607.81+400902.6	0.037	9.5	163.4	13.636	2	233	3.17	38.66	39.75	8.4
SDSS J121329.27+504429.4	0.031	96.5	574.2	12.825	1.87	277	3.04	39.5	40.12	8.7
SDSS J121951.65+282521.3	0.027	8.7	46.8	14.247	2.06	234	3.18	38.32	38.9	8.4
SDSS J122421.31+600641.2	0.044	6.1	57.7	14.043	2.04	283	3.46	38.61	39.44	8.7
SDSS J123011.85+470022.7	0.039	93.8	264	13.57	1.91	231	2.94	39.7	40	8.4
SDSS J124318.73+033300.6	0.048	63.5	211.5	14.31	1.94	223	3.13	39.71	40.08	8.3
SDSS J124633.75+115347.8	0.047	61.2	354.5	14.021	1.9	260	3.09	39.68	40.3	8.6
SDSS J125027.42+001345.6	0.047	54.5	310.1	15.38	1.73	196	3.35	39.62	40.23	8.1
SDSS J125409.12-011527.1	0.047	7.7	66.6	14.743	1.92	196	3.3	38.78	39.57	8.1
SDSS J130404.99+075428.4	0.046	10.5	128.2	13.618	1.97	278	3.18	38.89	39.84	8.7
SDSS J130837.91+434415.1	0.036	58.4	366.3	13.438	1.89	255	2.89	39.41	40.06	8.6
SDSS J133042.51+323249.0	0.034	17.9	218.5	14.256	1.85	179	3.3	38.85	39.79	7.9

Sources III

SDSS name	z	NVSS	[O III]	m_r	D_n	sigma_*	C_r	nu_L_r	L[OIII]	M_BH
SDSS J133455.94+134431.7	0.023	39.4	335.7	12.854	2.02	285	3.18	38.85	39.64	8.7
SDSS J133621.18+031951.0	0.023	30.4	258.8	13.28	1.96	212	3.22	38.73	39.52	8.2
SDSS J133737.49+155820.0	0.026	26.9	235.8	12.968	2.02	257	2.9	38.79	39.58	8.6
SDSS J134159.72+294653.5	0.045	10.4	81.8	14.463	1.85	196	3.02	38.87	39.62	8.1
SDSS J135036.01+334217.3	0.014	101.3	677.6	12.524	2	199	3.16	38.84	39.52	8.1
SDSS J135226.71+140528.5	0.023	25.5	133.5	12.971	2.07	307	3.4	38.66	39.23	8.9
SDSS J140528.32+304602.0	0.025	7.4	93.2	14.159	1.97	129	3.03	38.19	39.15	7.4
SDSS J141451.35+030751.2	0.025	26.7	370.8	13.025	1.88	207	3.13	38.76	39.76	8.2
SDSS J141517.98-022641.0	0.047	18.9	126.2	14.192	2.03	280	3.22	39.17	39.85	8.7
SDSS J142724.23+372817.0	0.032	20.8	72.5	13.721	2.05	301	3.43	38.87	39.27	8.8
SDSS J143156.59+164615.4	0.048	8.7	42.7	13.956	2.04	266	3.27	38.86	39.4	8.6
SDSS J143312.96+525747.3	0.047	15.6	93.3	15.076	1.57	232	3.35	39.09	39.72	8.4
SDSS J143424.79+024756.2	0.028	7.3	82.4	14.106	1.99	201	3.23	38.28	39.19	8.1
SDSS J143620.38+051951.5	0.029	18.7	212.1	13.337	1.97	284	3.35	38.73	39.64	8.7
SDSS J144745.52+132032.2	0.044	6.7	158.1	15.126	1.93	186	3.1	38.66	39.89	8
SDSS J145216.49+121711.5	0.031	8	76.7	14.222	1.94	188	3.23	38.43	39.26	8
SDSS J145243.25+165413.4	0.046	17.5	149.2	14.001	1.94	272	3.17	39.11	39.9	8.7
SDSS J145616.20+203120.6	0.045	25.8	65.1	13.922	1.98	326	3.35	39.25	39.51	9
SDSS J150152.30+174228.2	0.047	18.6	85	14.411	1.92	224	3	39.16	39.67	8.3
SDSS J150425.68+074929.7	0.049	7.8	54.5	14.979	2.04	226	3.13	38.82	39.52	8.3
SDSS J150601.89+084723.2	0.046	8.3	41.8	14.225	1.93	240	3.3	38.79	39.35	8.4
SDSS J150636.57+092618.3	0.028	27.8	73.9	14.329	1.68	141	2.94	38.87	39.15	7.5
SDSS J150808.25+265457.6	0.033	20.3	87.4	15.185	2	198	3.54	38.87	39.36	8.1
SDSS J152010.94+254319.3	0.034	18.3	120.9	13.756	2.05	263	3.41	38.85	39.52	8.6
SDSS J152151.85+074231.7	0.044	11.7	35.8	13.855	2.02	260	2.85	38.9	39.24	8.6
SDSS J153016.15+270551.0	0.033	13.3	195.8	14.309	1.85	205	3.08	38.69	39.71	8.2
SDSS J154147.28+453321.7	0.037	8.9	117.6	14.094	1.91	215	3.44	38.62	39.59	8.3
SDSS J154426.93+470024.2	0.038	17.6	177.5	13.642	1.98	264	3.11	38.94	39.8	8.6
SDSS J154451.23+433050.6	0.037	11.5	129.3	13.646	1.92	217	3.27	38.73	39.63	8.3
SDSS J155951.61+255626.3	0.045	144.7	43.3	14.516	1.89	252	3.18	40	39.33	8.5

Sources IV

SDSS name	z	NVSS	[O III]	m_r	D_n	sigma_*	C_r	nu_L_r	L[OIII]	M_BH
SDSS J155953.99+444232.4	0.042	59.5	158.9	14.474	1.89	182	3.26	39.56	39.84	8
SDSS J160426.51+174431.1	0.041	96	276.4	15.416	1.89	226	2.32	39.75	40.06	8.3
SDSS J160523.84+143851.6	0.041	8.6	55.8	13.705	2.01	259	3.04	38.7	39.36	8.6
SDSS J160641.83+084436.8	0.047	9.3	87.1	14.452	1.93	188	2.51	38.86	39.69	8
SDSS J161238.84+293836.9	0.032	27.4	147.3	14.036	1.93	242	3.44	38.99	39.57	8.5
SDSS J161256.85+095201.5	0.017	21.7	323.8	12.856	2.07	203	3.39	38.33	39.35	8.2
SDSS J162146.06+254914.4	0.048	9.1	70.9	14.168	1.95	198	2.94	38.87	39.61	8.1
SDSS J162846.13+252940.9	0.04	25.2	111.4	14.281	1.96	250	3.39	39.15	39.65	8.5
SDSS J162944.98+404841.6	0.029	7.7	77.9	16.542	1.98	263	2.14	38.36	39.21	8.6
SDSS J164925.86+360321.3	0.032	11.9	114.4	14.121	1.99	199	3.23	38.61	39.45	8.1
SDSS J165830.05+252324.9	0.033	13.1	181.9	14.326	1.93	219	3.43	38.68	39.68	8.3
SDSS J170358.49+241039.5	0.031	32.7	196.3	13.369	2.02	290	3.33	39.03	39.66	8.8
SDSS J171522.97+572440.2	0.027	57.2	174	12.56	1.97	292	2.81	39.16	39.5	8.8
SDSS J172215.41+304239.8	0.046	8.1	32.7	13.689	2.05	269	3.07	38.78	39.24	8.6

X-Ray Sources

SDSS name	Telescope	ObsID	Exposure (ks)	Offset (arcmin)
J004150.47−091811.2	Chandra	15173	42.5	3.4
J010101.12−002444.4	Chandra	8259	16.8	0
J011515.78+001248.4	XMM	404410201	54	0.095
J015127.10−083019.3	Swift	36976004	5.6	0.894
J080624.94+172503.7	Swift	85577001	1.3	0.337
J092405.30+141021.5	Chandra	11734	30.1	0
J093346.08+100909.0	Swift	36989002	12.2	1.867
J094319.15+361452.1	Swift	36997001	5.4	3.437
J104028.37+091057.1	XMM	38540401	24	0.003
J114232.84+262919.9	XMM	556560101	32.9	13.7
J115954.66+302726.9	Swift	90129001	3.4	2.803
J122206.54+134455.9	Swift	83911002	1.3	7.641
J125431.43+262040.6	Chandra	3074	5.8	2
Tol 1326−379	Swift	34308001	4.3	0
J135908.74+280121.3	Chandra	12283	10.1	3.1
J153901.66+353046.0	Swift	90113002	2.8	0.96
J160426.51+174431.1	Chandra	4996	22.1	2.5
J171522.97+572440.2	Chandra	4194	47.9	0
J235744.10−001029.9	XMM	–	–	–

Model parameter

Model Parameter

Table 1: Parameters of the SSC models. The following parameters are the same for all models: $\gamma'_{\mathrm{min}} = 100$, $p_1 = 2$, $p_2 = 3$, and $\theta = 20°$. The luminosity is given in logarithmic units $\log_{10}(L_i/(\mathrm{erg\,s^{-1}}))$, where a luminosity ratio between protons and electrons of $\xi = 10$ is assumed.

	$\mathrm{r'_{em}/cm}$	B'/G	Γ	γ'_{cut}	γ'_{max}	$u'_e/(\mathrm{erg\,cm^{-3}})$	$u'_\gamma/(\mathrm{erg\,cm^{-3}})$	L_{equ}	L_{CR}
Model A	1×10^{18}	1	2	2×10^{3}	5×10^{3}	1.29×10^{-7}	7.32×10^{-6}	46.8	46.5
Model B	5×10^{17}	0.1	2	1×10^{4}	2×10^{4}	3.05×10^{-5}	3.09×10^{-5}	44.2	44.16
Model C*	5×10^{16}	0.2	2	1×10^{4}	3×10^{4}	3.81×10^{-2}	1.80×10^{-2}	–**	44.92
Model D	1.7×10^{17}	0.06	1.2	1×10^{4}	3×10^{4}	2.67×10^{-3}	2.26×10^{-3}	–**	43.94
Model E	5×10^{17}	0.04	2	1×10^{4}	3×10^{4}	1.90×10^{-5}	3.39×10^{-6}	43.39	43.72
Model F	5×10^{17}	0.04	1.26	1×10^{4}	3×10^{4}	6.09×10^{-5}	1.11×10^{-5}	43.02	43.75

* For *model C* the second index is set to $p_2 = 4.8$.
** The equipartition scenario is only shown for $u'_B \gtrsim u'_e$.

Table 2: Parameters of the host galaxy model

	$L_{\mathrm{tot}}/(\mathrm{erg\,s^{-1}})$	T/K	$\epsilon_{\mathrm{dil}}/(\mathrm{cm^3\,erg^{-1}})$	R_e/kpc	m
blackbody	6.4×10^{44}	4801	0.29	1	4

Results for other models

Loss lengths

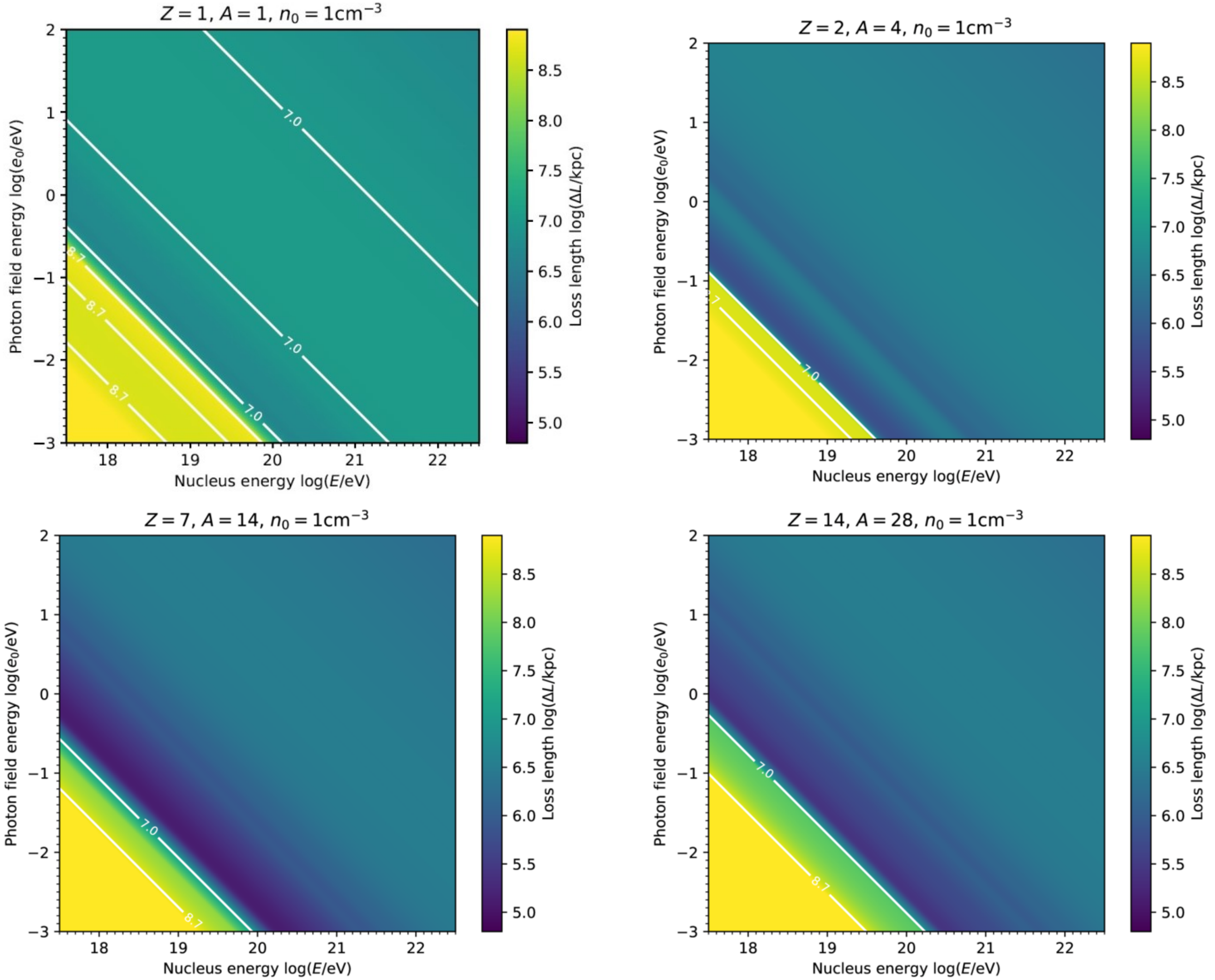

Maximum energies – Bohm

Table 3: Maximum Energy in the jet frame. Here the Bohm diffusion scenario is shown where the X-1 models are based on pure Fermi-I, and the X-2 models use the hybrid approach. The shock speed was fixed at $u_s = 0.1\,c$.

model	$\log_{10}(E'_{\rm max}/{\rm eV})$					$\langle\log_{10}(\zeta'_{\rm max}/{\rm V})\rangle$
	p	He	N	Si	Fe	
B-1	17.9	18.0	18.4	18.8	19.1	17.70 ± 0.11
C-1	17.1	17.3	17.6	17.9	18.3	16.90 ± 0.14
D-1	17.2	17.4	17.7	18.1	18.4	17.02 ± 0.12
E-1	17.4	17.8	18.3	18.6	18.8	17.44 ± 0.04
F-1	17.4	17.7	18.2	18.5	18.8	17.38 ± 0.02
B-2	19.2	19.5	20.0	20.3	20.6	19.18 ± 0.02
C-2	18.5	18.7	17.8	19.4	19.7	18.08 ± 0.57
D-2	17.2	17.4	17.8	18.1	18.4	17.04 ± 0.10
E-2	18.8	19.1	19.6	19.9	20.2	18.78 ± 0.02
F-2	17.6	17.9	18.3	18.7	18.9	17.54 ± 0.06

$\zeta = E/q$ is the rigidity of the particle in units of volt.

Merten et al. Astrop. Phys. **128** (2021) 102564

Maximum energies – Kolmogorov

Table C.4: Maximum energy in the jet frame. Here the Kolmogorov diffusion scenario ($\alpha = 1/3$) is considered where the X-1 models X-1 are based on pure Fermi-I acceleration, and the X-2 models use the hybrid approach. The shock speed was fixed at $u_s = 0.1\,c$.

model	$\log_{10}(E'_{\rm max}/{\rm eV})$					$\langle\log_{10}(\zeta'/{\rm V})\rangle$
	p	He	N	Si	Fe	
model B-1	14.5	14.8	15.3	15.6	15.9	14.48 ± 0.02
model C-1	13.8	14.1	14.6	14.9	15.2	13.78 ± 0.02
model D-1	13.8	14.1	14.7	15.0	15.2	13.82 ± 0.03
model E-1	14.1	14.4	14.9	15.2	15.5	14.08 ± 0.02
model F-1	14.1	14.4	14.9	15.6	15.5	14.16 ± 0.15
model B-2	19.2	19.5	19.9	20.3	20.6	19.16 ± 0.05
model C-2	18.5	18.7	18.7	19.2	19.5	18.18 ± 0.24
model D-2	14.0	14.3	14.9	15.2	15.4	14.01 ± 0.03
model E-2	18.8	19.1	19.6	19.9	20.2	18.78 ± 0.02
model F-2	14.4	14.7	15.3	15.6	15.8	14.42 ± 0.03